TRANSNAV
http://www.transnav.eu
the International Journal
on Marine Navigation
and Safety of Sea Transportation
Volume 17
Number 1
March 2023
DOI: 10.12716/1001.17.01.05

Model of the Random Phase of Signal E6 of the Galileo Satellite Navigation System

M. Džunda, S. Čikovský & L. Melníková
Technical University of Kosice, Kosice, Slovakia

ABSTRACT: The aim of this paper was to describe the random phase of the E6 signal, the Galileo satellite navigation system. Based on the available information, mathematical models of the measurement signals of the Galileo system were created. The frequencies of individual signals were determined and their structure visualized. A block diagram of the generation of individual signals is also shown. The main contribution of the paper is the creation of a random phase model of the E6 signal from the Galileo system. In accordance with the technical data of the Galileo system, the parameters of the random phase model were determined. The simulation results confirmed that the frequency instability of the continuous signal E6 ω_n received from the satellite is a stationary process. The short-term stability of the f_{FR} frequency ranges from 10^{-13} to 10^{-14}. The simulation results confirmed that the Doppler effect significantly affects the random phase of the E6 signal. This phenomenon can affect the results of navigation measurements using the E6 signal. The modeling and simulation results of the random phase of the E6 signal presented in the paper can be used to evaluate the immunity of the Galileo navigation system to interference.

1 INTRODUCTION

The Galileo satellite navigation system was launched as part of a joint project of the European Union and the European Space Agency. It is part of the Trans-European Transport Network, which aims to solve navigational and geographic issues. The Galileo project is an ambitious European venture aimed at creating the most advanced global positioning satellite system in the world. Its objectives are to create an autonomous system that provides guaranteed global positioning services, as well as interoperable compatibility with other global positioning systems, such as GPS and GLONASS. Galileo satellites permanently transmit three separate CDMA and right-hand circularly polarized (RHCP) signals, named E1, E5, and E6. Several studies and publications have been devoted to the analysis of the measurement signals of the Galileo system.

In the literature [1-2], models of measurement signals of some navigation systems are derived. The authors used these models to evaluate the accuracy of navigation systems. At the beginning of the system development, the system structure and signal models were described in the literature [3], where the author described the frequency plan and signal structure. The individual atmospheres of the Earth also have a great influence on the accuracy of signals. The author of the article [4] describes how signals behave when passing through the ionosphere. In the article [5], the author describes how it is possible to use more than three frequencies for decimeter positioning accuracy using Galileo and BeiDou signals. In the study [6], the authors investigated the positioning performance of

GPS L1/L2/L5 and Galileo E1/E5a/E5b/E6 in the conventional PPP mode and single epoch mode using uncombined coding and phase biases products generated at The National Center for Space Studies in France (CNES). The findings of the study revealed that by using uncalibrated phase and code biases, this multi-frequency code and phase measurements can be modeled in in undifferenced and uncombined form and ionosphere can be estimated. Galileo is currently developing new services designed to provide greater security and resistance to attacks, such as the Open Navigation Message Authentication Service (OS-NMA) and the Commercial Authentication Service (CAS). The authors [7] propose a robust and secure timing protocol independent of external time sources and at the end perform experimental tests to verify the proposed protocol. The study [8] is focused on accurate time transmission through the five-frequency uncombines Precise Point Positioning (PPP) Galileo system. The method that was used for the research is called the backward weighting method, based on which the short-term frequency stability and accuracy of the time transmission have been significantly improved. In the document [9], an analysis of Galileo clock and ephemeris broadcasts is performed with 43 months of data using the Galileo Receiver Independent Exchange (RINEX) consolidated navigation files from January 1, 2017, to July 31, 2020. Based on these observation results, the Galileo signal is evaluated in space and the probability of satellite failure is estimated. One of the main positioning errors is multipath interference. The improved Galileo signals are expected to provide greater resistance to multipath interference effects. The aim of the study [10], was to verify this hypothesis. The author's observation results confirm that Galileo codes are more resistant to the multipath interference effect than GPS codes. The basic performance limits of traditional two-step architectures of Global Navigation Satellite System (GNSS) receivers, which are directly related to the achievable time delay estimation performance, are analyzed in the article [11]. The authors of the article examine GPS signals L1 C/A, L1C, and L5, Galileo E1 OS, E6B, E5b-I, and E5 signals and Galileo meta-signals E5b-E6 and E5a-E6. The results show that The Alternative Binary offset carrier modulation (AltBOC) signals (Galileo E5 and meta-signals) can be used for accurate code-based positioning, which is a promising alternative to real-time carrier phase-based techniques. The author of the work [12] deals with the experimental analysis of positioning in a harsh environment, where he calculated parameters for horizontal and vertical position and speed. The analysis shows that GPS is not able to transmit continuous signals in a degraded environment, at the same time the Galileo system increases the availability of signals in such an environment. The authors of this article [13], investigated and analyzed the ionospheric delay estimation, based on two frequency GNSS signals. They focused on locations mainly in the middle latitudes of the Earth. As a result of the analysis, different ionospheric delay models can be used depending on the receiver position. There are different models of Galileo signals. Stochastic signal models are described in [14], which aimed to improve single-frequency GPS/Galileo signals. In addition, research was also devoted to the elevation angle and its effect on the satellite. Based on the stochastic models that have been outlined and used, it is possible to achieve a composite binary offset carrier (CBOC) signal are defined in [15] through tracking algorithms and simulations. The study provided an experimental as well as a theoretical analysis of the proposed algorithm for observing the Galileo E1 CBOC signal. In-band pulse interference of the E6 signal and its effect on the control tower (ATC) is discussed in the study [16]. Through the research, the authors found out that this type of interference poses a serious threat to GNSS users. Receiver problems related to data generation, modulation, and signal dispersion were investigated in [17]. The results achieved by the authors can contribute to the redesign of receivers and transmitters of the Galileo GNSS system. The authors of the document [18] compare the performance of GPS and Galileo signals against altitude. This comparison concluded that the Galileo system signal is up to 27% more accurate than the GPS system. The aim of the article [19] was the study of radio navigation signals of the Galileo system, which are transmitted by individual constellations of satellites, where the author represented individual power spectral densities, modulation schemes, and autocorrelation functions of the signals. The discovery of different signals through different GNSS constellations with amplitudes of millimeter series of station coordinates was described in the article [20], where the authors evaluated the contribution of the multi-constellation of the GLONASS, GPS, and Galileo systems. In this paper, the measurement signal models of the Galileo system, including the random phase model, are presented. The above-mentioned models can be used in the evaluation of the accuracy and resistance of the Galileo system to interference.

2 METHODOLOGY

In this chapter, we will focus on the mathematical analysis of the measurement signals of the Galileo system. It is important to know what types of modulation are used to generate individual GNSS Galileo signals. We focus on a detailed analysis of the signals. Galileo satellites transmit coherent navigation signals on three frequencies in the L band: E1, E5 and E6. Galileo transmits E6 on a carrier frequency of 1278.75 MHz that contains E6 components E6-A, E6-B and E6-C. The Galileo E5 signal — which is centred at 1191.795 MHz — contains E5a and E5b signals. E5a and E5b share a carrier frequency of 1191.795 MHz and 1176.45 is the center frequency of the E5a signal. E5a data and pilot components are located 15.345 MHz below the E5 carrier frequency. E5b signals can be monitored separately, because they are modulated on two different carrier frequencies in the E5 band [21]. Long codes allow monitoring of very weak signals, such as those received inside buildings, but are difficult to obtain because receivers detect signals by looking for delays in the received code, and long codes have more options than short codes. In addition to being good for quick fixes, shorter codes may lead to incorrect satellite positioning when the receiver exchanges signals with two satellites at the same time. Signal length may not be suitable for all types of users

(static users may prefer long codes, while, fast-moving users may prefer short codes). The answer is to offer substitute codes with distinct characteristics for various Galileo transmissions. One of the causes of the diversity of Gallieo signals naturally offers the possibility of ionospheric delay correction using suitable linear combinations. Of course, the ionospheric error causes a delay in the code range and a shift of the signal in the phase range. This causes the code ranges to be too long and uncorrected causes header errors in processed positions. If the position error is not corrected, this delay might make the distance between the user and the satellite as measured by the receiver appear to be much greater than it is. Thankfully, this delay varies according to the signal's frequency, with low-frequency delaying communications more than high-frequency signals. The ionospheric delay error can be removed from another measurement by merged values of all transmitted GNSS signals on at least 2 frequencies in order to correct the main ionospheric delay term by linear combination. The effectiveness of this cancellation will increase with the distance between the two frequencies. Galileo services are typically implemented as pairs of signals due to this [22].

2.1 *Signal E1*

The Galileo E1 signal is modulated by BOC, which is a binary offset carrier. BOC uses carrier shift modulation to shift the energy from the middle of the band away from the band. This is important because it allows the same band to be used for multiple GPS systems. BOC modulations use two independent design parameters. One is the carrier frequency of the auxiliary signal, fs, in MHz. The other is the code rate of code shift, fc, in mega chips per second. This gives the signal two parameters that can be used to manipulate the signal's power in specific ways. This is intended to reduce interference from other signals on the same band. Additionally, the redundant upper and lower sidebands of BOC modulations provide advantages in signal processing by receiver acquisition, carrier tracking, code tracking and data demodulation [23]. The entire transmitted Galileo E1 signal consists of the following components [27]:

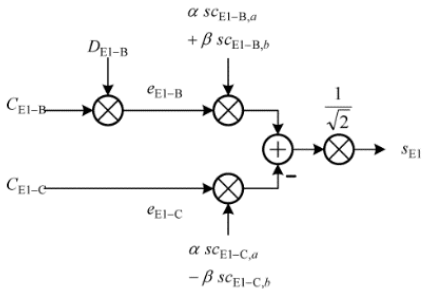

Figure 1. E1 signal modulation scheme [24].

Figure 1 shows the modulation scheme of signal E1. E1 open service data channel $e_{E1\text{-}B}(t)$ is generated from I / NAV navigation data stream $D_{E1\text{-}B}(t)$ and measurement code $C_{E1\text{-}B}(t)$, which are then modulated by subcarriers $SC_{E1\text{-}B,a}(t)$ and $SC_{E1\text{-}B,b}(t)$. The open service pilot channel E1 $e_{E1\text{-}C}(t)$ is generated from the range code $C_{E1\text{-}C}(t)$, including its secondary code, which is then modulated by subcarriers $SC_{E1\text{-}C,a}(t)$, and $SC_{E1\text{-}C,b}(t)$, in antiphase [27].

The Galileo E1 signal is modulated at a medium frequency such as [24]:

$$s(t) = A\left(C_D(t-\tau)\right) d_D(t-\tau)\, CBOC_-(t-\tau) + \\ - c_P(t-\tau)\, S_c(t-\tau)\, CBOC_+(t-\tau)\, x\cos\left(2\pi f_{IF} t + \theta\right) \quad (1)$$

where:

$$\boldsymbol{CBOC_-(t)} = \sqrt{10/11}\,\boldsymbol{BOC_1(t)} - \sqrt{1/10}\,\boldsymbol{BOC_6(t)} \quad (2)$$

$$CBOC_+(t) = \sqrt{10/11}\,BOC_1(t) + \sqrt{1/10}\,BOC_6(t) \quad (3)$$

$$BOC_x(t) = sign\left(\sin\left(x.2\pi.1.023e^6.t\right)\right) \quad (4)$$

A is the amplitude of the input signal at the input of the correlator,
C_P a C_D are extended sequences that carry pilot and data components,
d_D represents the navigation message symbol of the I / NAV modulated data component.
S_c represents the secondary code present on the pilot component,
τ is a sequence delay,
f_{IF} is the center frequency,
θ is the phase shift of the carrier frequency.

GPS C / A and Galileo BOC (1,1) share the L1 / E1 spectrum, which is shown in Figure 2. The mean frequency of the E1 / L1 signal is 1575.42 MHz. It is important to remember that the current E1 band was given the name L1 band for a long time, analogous to GPS, until 2008, when the name of the L1 signal was changed to the current E1.

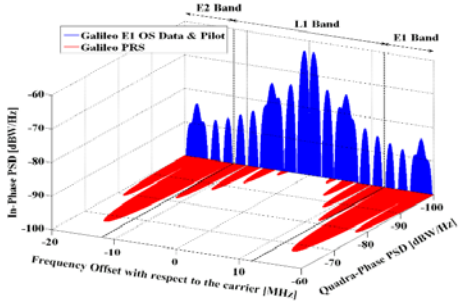

Figure 2. Structure of signal E1 [24].

Figure 2 shows that the carrier frequency of the E1 / L1 signal is centered on 0 MHz. The signal for PRS Galileo is shifted by 10 MHz to the right and -10 MHz to the left of the carrier frequency. The spectral power density of the E1 / L1 signal is -65 dBW.

2.2 *Signal E5*

The Galileo E5 signal consists of the signals E5a, E5b (and the modulation product signal) and is transmitted in the 1164 - 1215 MHz frequency band. Galileo satellites transmit navigation signals in the E5 band (1164-1215 MHz) using the AltBOC modulation

scheme. The E5 signal is modulated and multiplexed in AltBOC. Each of the recording and pilot channels are in-phase and quadrature components because they are signals in complex envelope format. These properties enable code range measurements at the centimeter level and allow for better mitigation of multipath effects [25]. The following Figure 3 shows the modulation of the E5 signal, which is modulated using the AltBOC modulation scheme.

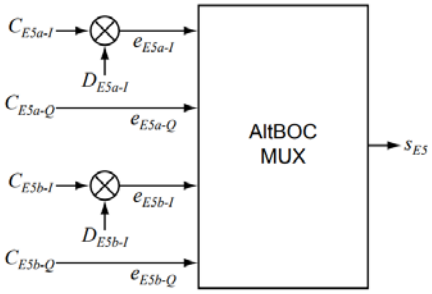

Figure 3. E5 signal modulation scheme [24].

The whole transmitted signal E5 consists of the following components [27]:
e_{E5a-I} from the F / NAV navigation data stream D_{E5a-I} modulated with the unencrypted measurement code C_{E5a-I}.
e_{E5a-Q} (pilot component) from unencrypted measurement code C_{E5a-Q}
e_{E5b-I} \ from the I / NAV navigation data stream D_{E5b-I} modulated by the unencrypted measurement code C_{E5b-I}.
e_{E5b-Q} (pilot component) from unencrypted measurement code C_{E5b-Q}.

The transmitted signal of the Galileo E5 system can be represented as [27]:

$$S_{E5_t}(t) = AR\left[S_{E5}(t)e^{j2\pi f_c t}\right] \tag{5}$$

$$S_{E5_t}(t) = S_{E5-I}(t) + jS_{E5-Q}(t), \tag{6}$$

where A is the amplitude of the signal; f_s is the carrier frequency that is selected as 1191.795 MHz; R is a real function.

The baseband envelope $S_{E5}(t)$ is given by [25]:

$$\begin{aligned} S_{E5}(t) = {} & \frac{1}{2\sqrt{2}}\left(e_{E5a-I}(t) + je_{E5a-Q}(t)\right)\left[SC_{E5-s}(t) - jSC_{E5-s}\left(t - \frac{T_{s,E5}}{4}\right)\right] + \\ & + \frac{1}{2\sqrt{2}}\left(e_{E5b-I}(t)\, je_{E5b-Q}(t)\right)\left[SC_{E5-s}(t) + jSC_{E5-s}\left(t\frac{T_{s,E5}}{4}\right)\right] + \\ & + \frac{1}{2\sqrt{2}}\left(\bar{e}_{E5a-I}(t)\, j\bar{e}_{E5a-Q}(t)\right)\left[SC_{E5-p}(t) - jSC_{E5-p}\left(t - \frac{T_{s,E5}}{4}\right)\right] + \\ & + \frac{1}{2\sqrt{2}}\left(\bar{e}_{E5b-I}(t) + j\bar{e}_{E5b-Q}(t)\right)\left[SC_{E5-p}(t) + jSC_{E5-p}\left(t - \frac{T_{s,E5}}{4}\right)\right] \end{aligned} \tag{7}$$

In this equation, the signal components e_{E5a-I}, e_{E5a-Q}, e_{E5b-I} a e_{E5b-Q} carry the navigation message codes. While the intermittent components e_{E5a-I}, e_{E5a-Q}, e_{E5b-I} and e_{E5b-Q} indicate signal products. Symbols SC_{E5-s} and SC_{E5-p} indicate the four-valued subcarrier functions for single-signal sidebands and product signal sidebands. The spectrum is divided into two side lobes, which are completely symmetrical due to the existence of subcarrier signals. These two lateral lobes are called E5a and E5b and are midway from the carrier frequency [25].

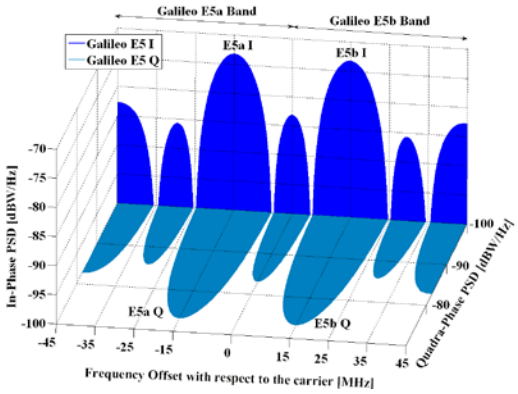

Figure 4. Structure of signal E5 [24].

Figure 4 shows that the signal power spectral density (PSD) is -80 dBW for Galileo channels E5a I and E5b I. For channels E5a Q and E5b Q, the PSD is -85 dBW. Channels E5a Q and E5b Q are shifted by -15MHz left and 15MHz right to the carrier frequency.

2.3 *Signal E6*

Galileo satellites use E6-B and E6-C radio navigation signals to identify their position. These signals are sent in the E6 band at 1278.75 MHz, and contain data and authentication. The data component of the E6-B signal is transmitted by each satellite at approximately 500 bits per second. The authentication is created using spread code encryption and is based on the satellites' precise positions. There are several benefits and drawbacks to this band of signals. One big advantage is the fact that this band is relatively new. One drawback is the presence of radio and radar interference. Additionally, this band of Galileo has higher bit rates than other bands. The E6 band is 1260-1300 MHz, and it contains two components: E6-B and E6-C. E6-B transmits 448 bits per second and E6-C transmits a pilot signal. E6 signals are using BPSK binary phase shift key technology at the signal level. The modulation scheme of the E6 signal is shown in Figure 5 [28]. The transmitted Galileo E6 signal consists of the following components, both (pilot and data components) being combined on the same carrier component, with 50 percent energy sharing [27]:

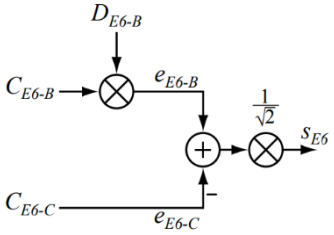

Figure 5. E6 signal modulation scheme [24].

e_{E6-B} from navigation data stream C / NAV D_{E6-B} modulated by encrypted measurement code C_{E6-B}
e_{E6-C} (pilot component) from the range code C_{E6-C} [25].

The E6 signal is generated by a combination of components B and C according to the equation [25]:

$$S_{E6}(t) = \frac{1}{\sqrt{2}}\left[e_{E6-B}(t) - e_{E6-C}(t)\right], \quad (8)$$

where

$$e_{E6-B}(t) = \sum_{-\infty}^{+\infty}\left[C_{E6-B,|i|_{L_{E6-B}}} d_{E6-B,[i]_{DC_{E6-B}}} rect_{T_{C,E6-B}}(t) - iT_{C,E6-B}\right], \quad (9)$$

$$e_{E6-C}(t) = \sum_{-\infty}^{+\infty}\left[C_{E6-C,|i|_{L_{E6-C}}} rect_{T_{C,E6-C}}(t) - iT_{C,E6-C}\right] \quad (10)$$

$D_{E6\text{-}B}$ is the navigation data flow of the C / NAV of component B,
$C_{E6\text{-}B}$ is the range code of component B,
$C_{E6\text{-}C}$ is the range code including its secondary component code C,
$e_{E6\text{-}B}(t)$ is a binary navigation signal, modulated by component B, including range code, sub-carrier, and navigation message data. $(e_{E6\text{-}B}(t) = C_{E6\text{-}B}(t)D_{E6\text{-}B}(t))$,
$rect_{Tc}(t)$ is a rectangular function that equals 1 for 0 <t <T and equals 0,
$[i]_{DC\ E6\text{-}B}$: is an integer part of $i/DC_{E1\text{-}B}$,
$T_{C,E6\text{-}B}$ is the length of the component B measurement code chip (second),
$e_{E6\text{-}C}(t)$: is a binary navigation signal, modulated by component C, including range code and subcarrier. $(e_{E6\text{-}C}(t)) = C_{E6\text{-}C}(t)$.

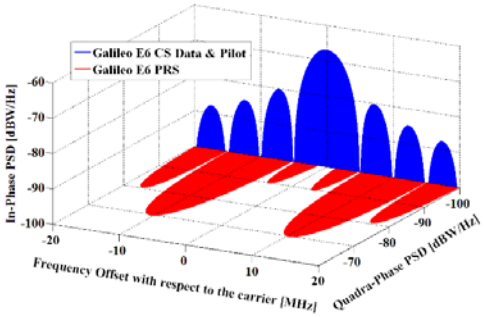

Figure 6. Structure of signal E6 [24].

It can be seen from Figure 6 that the PSD of the signal E6 is -70 dBW. The Galileo PRS channel is shifted by 10Mhz to the right and at the same time by -10Mhz to the left of the carrier frequency and has a value of -70 dbW. GNSS receivers use Direct Sequence Spread Spectrum (DSSS) modulation features to collect signals from multiple satellites and process them independently. The independent processing of the various signals is based on quasi-orthogonal codes used to modulate the various components of the signal. For this reason, the signal from one satellite will be considered in the following equation. The continuous signal received from the satellite can be modelled as the sum of L useful components, which can be expressed as [29]:

$$y(t) = \sum_{j=0}^{L-1}\sqrt{2C_j}e_j(t-\tau_j)\cos(2\pi(f_{FR,j} + f_j)t + \varphi j) + n(t), \quad (11)$$

Where L is the total number of signals transmitted by the satellite. The expressions $e_j(t)$ represent the various components of the GNSS baseband signal modulated by the propagating code and carrying the navigation message. For each signal component identified by the subscript j, C_j, the power is received and $f_{FR,j}$ is the center frequency, while τ_j, φ_j and f_j the code delay, carrier phase and Doppler shift introduced by the propagation channel. Finally, $n(t)$ is the zero average additive white Gaussian noise (AWGN) introduced by the propagation channel and with a spectral density N_0. The signal power ratio, C_j and N_0, defines the power-to-noise spectral density ratio (C/N0), one of the main signal quality indicators used in GNSS signal processing.

When only Galileo E6-B / C signals are considered, the signal can be expressed as [28]:

$$y_{E6}(t) = \left[\sqrt{2C_D}e_{E6-B}(t-\tau_0) - \sqrt{2C_p}e_{E6-C}(t-\tau_0)\right] \cdot \cos(2\pi(f_{RF,E6} + f_0)t + (t) + n(t) \quad (12)$$

where $\varphi(t)$ is random phase of signal E6.

This signal is given by a combination of pilot and data components, which have the same power [29]:

$$C_D = C_P = D \quad (13)$$

3 RESULTS

In some tasks of the analysis and synthesis of satellite navigation systems, it is necessary to create models of the measurement signals of these systems and their parameters. In this paper, models of the measurement signals of the Galileo satellite navigation system have been presented. One of the parameters of the developed signal model $y(t)$, which is described by relation (11), is the random phase of this signal $\varphi_j(t)$

3.1 *The random phase model of the signal E6 received from the satellite*

The random phase model of the signal E6 received from the satellite

The change in the signal y(t) phase may be due to the instability of the control signal generator due to thermal noise of its elements. We consider the random phase $\varphi_j(t)$ from relation (11) to be a diffusion process, which we can express in the form:

$$\frac{\varphi(t)}{dt} = n_F(t) \quad (14)$$

The spectral power density of the $n_F(t)$; process can be assumed to be constant over the entire Galileo receiver bandwidth. Therefore, we approximate the $n_F(t)$; process by white Gaussian noise with known characteristics:

$$E(n_F(t)) = 0;\ E(n_F(t_1)\cdot n_F(t_2)) = \frac{N_0}{2}\cdot\delta(t_2 - t_1) \quad (15)$$

where N_0=*const*. is the power spectral density of the process $n_F(t)$.

We consider the initial phase $\varphi_j(0)$ to be random, having a uniform probability distribution on the interval [$-\pi$, π]. The variance of the phase σ_φ^2 increases with time therefore the random phase $\varphi(t)$ is a non-stationary process. Fluctuations in the phase of the received signal (11) may be caused by a change in the frequency ω_0 of the signal generator, for example, due to a change in the external conditions of its operation. This change can be described by the stochastic differential equation:

$$\frac{d\omega_n}{dt} = -\gamma_\omega \cdot \omega_n + \left(2 \cdot \gamma_\omega \cdot \sigma_{\omega n}^{\ 2}\right)^{0.5} \cdot n_\omega(t), \qquad (16)$$

where ω_n — expresses the instability of the frequency of the continuous signal received from the satellite $y(t)$; $n_\omega(t)$—white Gauss noise with zero mean value and an intensity equaling to one; γ_ω^{-1}—is the time of correlation of processes ω_n; $\sigma_{\omega n}^2$—dispersion of the $y(t)$ signal frequency fluctuation.

Among the serious factors that affect the phase change of the useful signal $y(t)$ is the Doppler effect which manifests itself as a shift of the carrier frequency $f_{FR,j}$ by the value of Ω_D .

$$\Omega_D = \left(\frac{\Omega_0}{c}\right) \times \frac{dD(t)}{dt}, \qquad (17)$$

where $dD(t)/dt$ is the radial component of the Galileo receiver velocity.

In accordance with relations (11), (16) and (17), the phase fluctuations of the useful signal $y(t)$ can be described by the relation:

$$\frac{d\varphi}{dt} = \omega_n - \left(\frac{\Omega_0}{c}\right) \times \frac{dD(t)}{dt} + \left(\frac{N\varphi}{2}\right)^{0.5}, \qquad (18)$$

where $D_F = N\varphi/2\ \gamma_\omega$ is the dispersion of the random phase $\varphi_j(t)$ of the signal $y(t)$ during the correlation time of the process ω_n.

The process ω_n is stationary, although its nature depends on the specification of the initial conditions for equation (16). We can model the random signal phase $y(t)$ using relations (16) to (18).

4 DISCUSSION

The random phase model, which is determined by equations (16) to (18), was verified by simulation. During the simulations, it was necessary to set the parameters of the model so that they were consistent with the parameters of the E6 signal. Some parameters of the Galileo satellite navigation system signals are analysed in [31]. The authors of this work investigated the accuracy of single-frequency time and frequency transmission using Galileo observations. Based on the results of this work, the parameters of the random phase model during simulations were determined in the following way. The mean frequency of signal E6 was equal to = 1278.75 MHz. Parameter γ_ω=0.032 s^{-1}. $\sigma_{\omega n}^2$ - dispersion of the $y(t)$ signal frequency fluctuation was equal to 2.56x10^{-4}°^{2}s^{-2}. The dispersion of the random phase $\varphi_j(t)$ of the signal $y(t)$ during the correlation time of the process ω_n was equal to: DF = 0.032°^{2}. The instability of the frequency of the continuous signal received from the satellite $\omega_n(t_0)$ = 0.0°s^{-1}. Phase fluctuations of the useful signal $\varphi_j(t_0)$ = 0.0°. $n_\omega(t)$ - white Gauss noise with zero mean value and an intensity equal to one. The Doppler effect was simulated using a dynamic model of the flying object movement presented in [2]. Simulations were also performed without considering the influence of the Doppler effect. The simulation results are shown in figures 7 to 11.

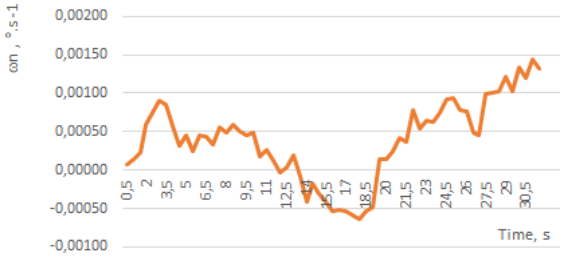

Figure 7. The dependence of the frequency ω_n on time.

Figure 7 shows the dependence of frequency ω_n on time. The simulation results have confirmed that the created model describes the E6 signal generator from the Galileo system quite accurately. The short-term relative stability of the frequency $f_{FR,j}$ ranges from 10^{-13} to 10^{-14}. The simulation results confirmed that the process ω_n is stationary.

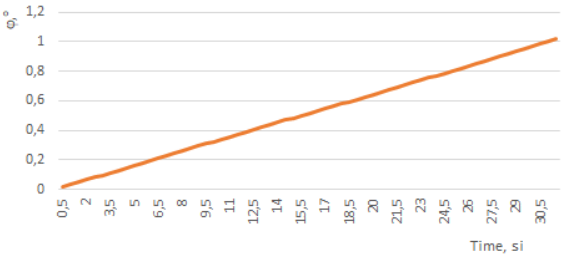

Figure 8. Dependence of the random phase φ_j on time without the influence of the Doppler effect.

Figure 8 shows the dependence of the random phase φ_j on time without the influence of the Doppler effect. It is clear from the figure that the random phase of the signal changes with time almost linearly in the range from 0 to 1.0°. This is because the E6 signal generator is stable.

Figure 9. Dependence of the random phase φ_j on time for a receiver movement speed of 1.0 m.s^{-1}.

The simulation results shown in Figure 9 confirm that the Doppler effect is applied during the movement of the receiver of the Galileo system, which causes the fluctuation of the random phase φ_j. We assume that the process φ_j is stationary.

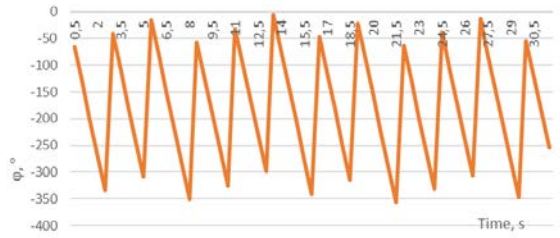

Figure 10. Dependence of the random phase φ_j on time for movement speed of 5.0 m.s^{-1}.

Furthermore, a simulation of the dependence of the random phase φ_j was performed for the receiver movement speed of 5.0 and 10.0 m.s-1. The simulation results are shown in figures 10 and 11.

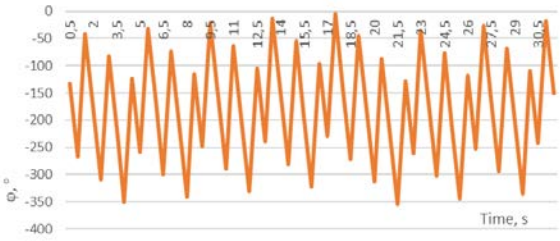

Figure 11. Dependence of the random phase φ_j on time for receiver movement speed of 10.0 m.s^{-1}.

From figures 10 and 11, the Doppler effect significantly affects the phase fluctuations of the E6 signal. Therefore, it is necessary to take this effect into account in measurements using the E6 signal, as it can cause large measurement errors.

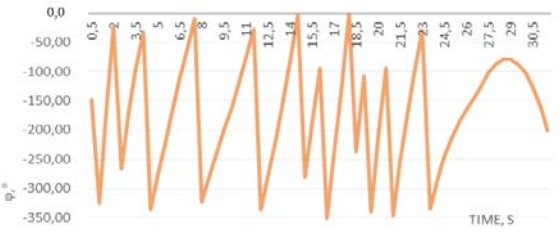

Figure 12. Dependence of the random phase φ_j on time when placing the receiver on board of a flying object.

The dependence of the random phase φ_j on time during the movement of a receiver, which is on board of the flying object, is shown in fig. 12. The movement of the flying object was modelled by the dynamic model presented in [2]. The speed of the flying object was 265.0 m.s^{-1}. Its acceleration was 5.0 m.s^{-2}. The simulation results have confirmed that the Doppler effect significantly affects the random phase of the E6 signal. This phenomenon can affect the results of navigation measurements using the E6 signal. Therefore, it is necessary to take into account the influence of the Doppler effect when synthesizing the receiver for processing signals of the Galileo system.

Based on the simulation results, the continuous signal $y(t)$ (11) received from the satellite can be expressed as :

$$y(t) = \sum_{j=0}^{L-1} \sqrt{2C_j e_j}\,(t-\tau_j)\cos(2\pi(f_{FR,j})t + \varphi j) + n(t) \qquad (19)$$

In this model, the Doppler effect is included in the phase φ_j (18) model.

5 CONCLUSIONS

In this article, we analyse selected parameters of the Galileo satellite navigation system signal. Based on the available information, mathematical models of the measurement signals of the Galileo system were created. The frequencies of individual signals were determined, and their structure visualized. Also shown is the block diagram of the generation of individual signals. The results of the modelling of the Galileo system signals, which are presented in the paper, can be used to evaluate the resistance of the Galileo navigation system to interference. The given images of the Galileo system signals allow a better understanding of the structures of the individual signals. The modelling results confirm that the Galileo system signals have a different structure and a different frequency spectrum. In further research, it will be possible to use Galileo signal models to simulate the effect of intentional jamming on Galileo accuracy. Also, for modelling the influence of the atmosphere on the propagation of measurement signals of the Galileo system. Furthermore, it will be possible to monitor the debasement of measurement signals when they are received by navigation receivers of the Galileo system. Due to the modulations used in the Galileo system, it is believed that the signals of the Galileo system may in the future enable more accurate positioning compared to other satellite systems. This advantage should be manifested mainly in dense urban development or in forest stands. An important advantage of the Galileo system is the use of a dual frequency for measuring the position of the user of the Galileo system. The Galileo system is also expected to be more resistant to interference. A shortcoming of the mentioned signal models is the absence of a more detailed description of the random phase of these signals. In our research we focused on modelling the random phase of the Galileo navigation system signals. One of the parameters of the constructed signal model $y(t)$, which is described by the relation (11), is the random phase of this signal $\varphi_j(t)$. The change in the signal $y(t)$ phase may be due to the instability of the control signal generator due to the thermal noise of its elements. Also due to a change in the external operating conditions of the carrier signal generator. As mentioned, the random phase is affected by the Doppler effect. All the above effects on the random phase $\varphi_j(t)$. of the measurement signal $y(t)$ are considered in the development of the model which is described by relations (16) to (18). In accordance with the technical data of the Galileo system, the parameters of the random phase model were determined. The simulation results confirmed that the instability of the frequency of the continuous signal E6 ω_n received from the satellite is a stationary process. The short-term stability of the frequency $f_{FR,j}$ ranges from 10^{-13} to 10^{-14}. The simulation results have confirmed that the Doppler effect significantly affects the random phase of the E6 signal. This phenomenon can affect the decoding of information from the E6 signal, which will be reflected in the results of

navigation measurements. The above model of the random phase $\varphi_j(t)$ of the measurement signal $y(t)$ can be used to assess the accuracy and resistance of the Galileo satellite navigation system against interference.

REFERENCES

[1] Dzunda, M; Kotianova, N; Dzurovčin, P. Selected Aspects of Using the Telemetry Method in Synthesis of RelNav System for Air Traffic Control. International journal of environmental research and public health 17 (1), Jan 2020

[2] Dzunda, M; Dzurovcin, P. Selected Aspects of Navigation System Synthesis for Increased Flight Safety, Protection of Human Lives, and Health. International journal of environmental research and public health 17 (5), Mar 2020,

[3] Hein, Guenter W., Godet, Jeremie, Issler, Jean-Luc, Martin, Jean-Christophe, Lucas-Rodriguez, Rafael, Pratt, Tony, "The GALILEO Frequency Structure and Signal Design," Proceedings of the 14th International Technical Meeting of the Satellite Division of The Institute of Navigation (ION GPS 2001), Salt Lake City, UT, September 2001, pp. 1273-1282.

[4] Bidaine, Benoît. Ionosphere Crossing of Galileo Signals, 2006.

[5] Geng, Jianghui, and Jiang Guo. "Beyond three frequencies: An extendable model for single-epoch decimeter-level point positioning by exploiting Galileo and BeiDou-3 signals." Journal of Geodesy, 2020, 94.1, pp. 1-15.

[6] Zhao, Lei, Paul Blunt, and Lei Yang. Performance Analysis of Zero-Difference GPS L1/L2/L5 and Galileo E1/E5a/E5b/E6 Point Positioning Using CNES Uncombined Bias Products. Remote Sensing, 2020, 14.3, pp. 650.

[7] Ardizzon, Francesco. Authenticated Timing Protocol Based on Galileo ACAS. Sensors 2022, 22.16, pp. 6298.

[8] Liu, Gen, Xiaohong Zhang, and Pan Li. "Improving the performance of Galileo uncombined precise point positioning ambiguity resolution using triple-frequency observations." Remote Sensing 11.3 (2019): 341.

[9] Alonso, María Teresa, et al. "Galileo Broadcast Ephemeris and Clock Errors Analysis: 1 January 2017 to 31 July 2020." Sensors 20.23 (2020): 6832.

[10] Prochniewicz, Dominik, and Maciej Grzymala. "Analysis of the impact of multipath on Galileo system measurements." Remote Sensing 13.12 (2021): 2295.

[11] Das, Priyanka, Lorenzo Ortega, Jordi Vilà-Valls, François Vincent, Eric Chaumette, and Loïc Davain. "Performance limits of GNSS code-based precise positioning: GPS, galileo & meta-signals." Sensors 20, 2020, no. 8 , pp. 2196.

[12] Borio, Daniele, and Ciro Gioia. "Galileo: The added value for integrity in harsh environments." Sensors 16.1 (2016): 111.

[13] J Julien, Olivier, Christophe Macabiau, and Jean-Luc Issler. "Ionospheric delay estimation strategies using Galileo E5 signals only." In Proceedings of the 22nd International Technical Meeting of The Satellite Division of the Institute of Navigation (ION GNSS 2009), pp. 3128-3141. 2009.

[14] Afifi, Akram, and Ahmed El-Rabbany. Stochastic modeling of Galileo E1 and E5a signals.International Journal of Engineering and Innovative Technology (IJEIT) 3.6, 2013, pp. 188-192.

[15] Jovanovic, Aleksandar, Cécile Mongrédien, Youssef Tawk, Cyril Botteron, and Pierre-André Farine. "Two-step Galileo E1 CBOC tracking algorithm: when reliability and robustness are keys!." International Journal of Navigation and Observation2012 (2012).

[16] Arribas, Javier, Jordi Vilà - Valls, Antonio Ramos, Carles Fernández - Prades, and Pau Closas. Air traffic control radar interference event in the Galileo E6 band: Detection and localization. Navigation 66 2019, no. 3, pp. 505-522.

[17] Setlak, Lucjan, and Rafał Kowalik. E1 Signal Processing of the Galileo System in the Navigation Receiver. Communications-Scientific letters of the University of Zilina, 2021, 23.3, E46-E55.

[18] Pascual, Daniel, Hyuk Park, Adriano Camps, A. Alonso, and Raul Onrubia. "Comparison of GPS L1 and Galileo E1 signals for GNSS-R ocean altimetry." In 2013 IEEE International Geoscience and Remote Sensing Symposium-IGARSS, pp. 358-361. IEEE, 2013.

[19] Hein, Guenter W., J. Godet, Jean-Luc Issler, Jean-Christophe Martin, Rafael Lucas-Rodriguez and Tony Pratt. The GALILEO Frequency Structure and Signal Design. (2001).

[20] Sośnica, Krzysztof, Radosław Zajdel, Grzegorz Bury, Kamil Kazmierski, Tomasz Hadaś, Marcin Mikoś, Maciej Lackowski, and Dariusz Strugarek. Contribution of the Galileo system to space geodesy and fundamental physics. No. EGU22-2477. Copernicus Meetings, 2022.

[21] Galileo navigation signals and frequencies . Available online: https://www.esa.int/Applications/Navigation/Galileo/Galileo_navigation_signals_and_frequencies (accessed on 03.11.2022).

[22] EUROPEAN GNSS (GALILEO) OPEN SERVICE SIGNAL-IN-SPACE INTERFACE CONTROL DOCUMENT Issue 2.0, January 2021 (accessed on 03.11.2022).

[23] Olivier Julien, Christophe Macabiau, Emmanuel Bertrand. Analysis of Galileo E1 OS unbiased BOC/CBOC tracking techniques for mass market applications. NAVITEC, 5th ESA Workshop on Satellite Navigation Technologies and European Workshop on GNSS Signals, Noordwijk, Netherlands, DEC 2010, pp 1-8, 10.1109/NAVITEC.2010.5708070. hal-01022203

[24] European Commission (2010), European GNSS (Galileo) Open Service – Signal-In-Space Interface Control Document Issue 1, February.

[25] Khan, Subhan & Jawad, Muhammad & Safder, Muhammad & Jaffery, Mujtaba & Javid, Salman. Analysis of the satellite navigational data in the Baseband signal processing of Galileo E5 AltBOC signal. Arctic, 2018, 71. 2-17.

[26] Maufroid, Xavier, Jesús Cegarra, José Caro, Laura García, and Chiara Scaleggi. The Galileo Return Link Service Provider in the Works. In Proceedings of the 30th International Technical Meeting of the Satellite Division of The Institute of Navigation (ION GNSS+ 2017), pp. 1333-1346. 2017.

[27] J.A Ávila Rodríguez, Galileo Signal Plan, University FAF Munich, Germany, 2011

[28] Maufroid, Xavier, Jesús Cegarra, José Caro, Laura García, and Chiara Scaleggi. "The Galileo Return Link Service Provider in the Works." In Proceedings of the 30th International Technical Meeting of the Satellite Division of The Institute of Navigation (ION GNSS+ 2017), pp. 1333-1346. 2017.

[29] Elhawary, M., Gomah, G., Zekry, A., & Hafez, I. Simulation of the E1 and E6 Galileo Signals using SIMULINK. International Journal of Computer Applications, 2014, 88(15), 41–48. https://doi.org/10.5120/15431-4043

[30] Galileo Signal Plan - Navipedia. Available from: https://gssc.esa.int/navipedia/index.php/Galileo_Signal_Plan (accessed on 03.11.2022).

[31] Xu, W.; Yan, C.; Chen, J. Investigation of Precise Single-Frequency Time and Frequency Transfer with Galileo E1/E5a/E5b/E5/E6 Observations. Remote Sens. 2022, 14, 5371. https://doi.org/10.3390/rs14215371.